Materials Science-Poland
Volume 43 Issue 1 · pp. 18–41 · DOI: 10.2478/msp-2025-0003

Materials Science-Poland

Development of a sustainable geopolymeric grout via mechanochemical activation with recycled brick powder

Research Article

Altuğ Saygılı[1], Ahmed Ali Agha[1,2], Mukhtar Hamid Abed[3,4]*

[1] Department of Civil Engineering, Muğla Sıtkı Koçman University, Muğla, Turkey
[2] North Refineries Company, Baiji, Iraq
[3] Department of Civil Engineering, Dijlah University College, Baghdad, Iraq
[4] Projects Department, Al Ramadi Municipality, Anbar Province, Iraq

Received 25 November 2024; Accepted 17 January 2025

Abstract: This research aims to address the limitations of conventional geopolymerization techniques in developing an environmentally friendly mechanochemically activated geopolymeric (MG) grout. The study primarily focuses on assessing the feasibility of using recycled waste brick powder (WBP) as a substitute for traditional industrial waste materials, such as ground granulated blast furnace slag (GGBS). A comparative analysis with the conventionally activated geopolymer (CG) grout was conducted to establish benchmarks for evaluating activation mechanisms. Key performance indicators, including mini-slump flow, setting time, unconfined compressive strength, density, and stress–strain behavior, were evaluated. Microstructural properties were analyzed using X-ray diffraction and scanning electron microscopy. Experimental results revealed that incorporating WBP as a partial replacement for GGBS significantly influenced both fresh and mechanical properties of the geopolymer grout. Substituting 15–45% of GGBS with WBP increased the slump flow of MG from 8.5 to 10 cm, reduced the final setting time from 235 to 90 min, and enhanced the compressive strength from 4.3 to 14 for 90 days, highlighting the potential of WBP as an effective supplementary material in sustainable grout formulations. The mechanochemical activation process further improved the performance, reducing the mini-slump flow by 10–27% and the final setting time by 9–25% and increasing the compressive strength by 7–30% compared to conventional activation methods. Microstructural analysis indicated that the pure WBP-based geopolymer grout exhibited a loose and fragmented morphology. However, the substitution of 15–45% GGBS for WBP resulted in more compact and homogeneous microstructures, with the MG grout showing greater density and compaction than CG. These findings demonstrate the efficacy of MGs incorporating WBP as a sustainable and high-performance alternative for grouting applications.

Keywords: *Mechanochemical activation • Geopolymer • Waste brick powder • Grouting • Ground granulated blast furnace slag*

1. Introduction

Grouting serves as a highly effective technique for ground improvement in the construction sector and is employed in diverse applications such as tunnels, anchors, dam barriers, pre-stressed coating cables, and building foundations. Ordinary Portland cement (OPC) is the most widely used binder for grouts in the modern construction industry. However, the extensive carbon emission associated with OPC production poses a significant environmental concern, with the cement industry contributing approximately 7% of all carbon dioxide (CO_2) emissions. Notably, an estimated 0.8–1.0 tons of CO_2 are emitted into the atmosphere during the production of 1 ton of OPC [1]. As a result, there has been a considerable focus on exploring substitutes for cement in scientific studies. One alternative is using geopolymers as a binder, which results in a 60–80% reduction in CO_2 emissions and a 60% decrease in energy consumption during production compared to OPC [2]. In addition, geopolymers offer numerous advantages such as early strength [3], rapid hardening [4], low shrinkage [5], reduced permeability [6],

* E-mail: eng.mukhtar92@gmail.com

Open Access. © 2025 Altuğ Saygılı *et al.*, published by Sciendo
This work is licensed under the Creative Commons Attribution-NonCommercial-NoDerivs 4.0 License.

control over humidity and temperature, high resistance to chemical corrosion [7], and fire resistance [8].

Despite the geopolymer binder's excellent environmental potential, which promotes its employment as a prospective alternative stabilizer to Portland cement, geopolymer utilization has been restricted to small-scale applications until recently. In order to promote the environmental friendliness of geopolymers and encourage their use in soil stabilization, it is important to address certain challenges associated with their production. The conventional process for generating geopolymers usually calls for the use of solid aluminosilicate precursors and alkaline solutions [9]. These alkaline solutions, which often contain hazardous activators such as potassium hydroxide or sodium hydroxide (NaOH), play a crucial role in dissolving the raw materials and controlling the mechanical characteristics of the resulting geopolymer binder [10,11]. The process of dissolving NaOH in water, which is an important stage in the conventional procedure, produces an aggressive alkaline environment and poses considerable difficulties in terms of handling and safety concerns in construction sites [12,13]. Hence, it is imperative to devise an alternate way of activation that may surmount these constraints and enable the utilization of geopolymeric materials in the solid state, akin to OPC. The application of solid-form geopolymers offers a novel solution for addressing the difficulties linked to traditional two-part geopolymeric systems. This approach obviates the need to deal with aggressive alkaline solutions for geopolymer activation. By investigating alternative methods of activating geopolymers, it may be possible to improve their ecological sustainability, practicality, and widespread use in the building industry [14]. This shift toward solid-form geopolymers offers a promising avenue to promote the safe and efficient utilization of geopolymeric materials in soil stabilization applications.

Mechanochemical activation represents a novel approach to producing geopolymers utilizing a solid-state chemistry mechanism. This method entails mechanically milling or grinding finely divided solid particles, which develops densely molecular, reactive, and non-crystalline composite particles [14,15]. The mechanochemical activation induces structural transformations and enhances the reactivity of the particles, leading to the formation of geopolymers with improved properties [13,16,17]. The process entails co-grinding solid binders, including aluminosilicate sources (e.g., fly ash, rice husk ash), with solid alkali activators (e.g., NaOH and sodium silicate) in a ball mill. Consequently, water is the sole element necessary for initiating the process of geopolymerization reaction [17,18]. Recent studies have shown that the mechanochemical activation process has the potential to enhance reactivity, modify the structure of polymerized units, and significantly improve the mechanical characteristics of geopolymeric products [15,18–20]. According to the findings of Hosseini et al. [17], the mechanochemical synthesis process improves fly ash-bottom ash particle dispersion, modifies the chemical reactions of aluminosilicate and alkali activators, increases the interconnectivity of the geopolymer structure, and decreases the pore size. As a consequence, the mechanical properties of the material would improve by 60–80%.

While past studies had only examined fly ash and ground granulated blast furnace slag (GGBS) mechanochemical geopolymers, the utilization of traditional aluminosilicate materials, such as fly ash, GGBS, and metakaolin, has become increasingly challenging due to industry competition, uneven regional distribution, and restrictions on coal and combustion processes [21,22]. Consequently, there has been growing interest in employing recycled brick/concrete aggregate and powder in geopolymer production [23]. This approach can reduce carbon emissions, dependence on traditional aluminosilicates, and accumulation of construction and demolition wastes (CDWs) [24]. The brick and concrete waste in C&D waste is more than 80% of the total CDW in China, the United States, and India, generating 2,360 million, 600 million, and 350 million tons of CDW in 2018, respectively [25,26].

The literature has documented several intriguing efforts entailing the utilization and recycling of demolition and construction wastes like ceramic and brick wastes as pozzolanic materials [23,27–29]. Figiela et al. [30] investigated the partial replacement of metakaolin and fly ash with clay bricks and concrete debris in the production of geopolymers. The study demonstrated the feasibility of manufacturing construction materials using industrial byproducts such as fly ash and CDW. Alghamdi et al. [31] developed high-performance alkali-activated materials (AAMs) by incorporating waste recycled brick powder (WRBP) as a binder and filler. Partial replacement of binary blends (ground granulated blast furnace slag [GGBFS] and metakaolin) and fine aggregates (silica sand) with WRBP significantly influenced the workability, strengths, surface morphology, and microstructure of the AAMs. The study concluded that utilizing WRBP in cement-free AAMs offers environmental benefits by reducing landfill waste and promoting sustainability in construction industries. Abadel et al. [32] investigated incorporating dehydrated cement powder (DCP) as a partial replacement for GGBFS in alkali-activated slag-based mixtures. Their systematic preparation and classification of novel mixtures demonstrated that DCP and red mud (RM) enhance the mechanical and durability properties while meeting sustainability goals in the construction sector. Additionally, Rakhimova and Rakhimov [33] investigated the potential of incorporating waste brick powder (WBP) in the production of alkali-

activated cement, with a 20% increase in GGBS. A review by Zhu and Zhu [34] and Tang et al. [26] of published studies examined the use of recycled brick powder (RBP) and recycled concrete powder (RCP) as substitutes. These studies found that using high replacement ratios of WBP and/or RCP can significantly decrease the mechanical properties of concrete. For instance, Xiao et al. [35] reported a 25.3% decrease in the strength performance of mixtures when 45% of the binder was replaced with WBP and RCP. Conversely, at low replacement ratios, incorporating WBP and/or RCP in concrete may result in higher compressive strength and better durability than the conventional concrete.

The existing literature highlights a significant research gap in the performance evaluation of WBP-based geopolymers activated through mechanochemical processes. To address this gap, the present study investigates the feasibility and effectiveness of a novel mechanochemically activated geopolymeric (MG) grout that incorporates recycled WBP as a sustainable alternative to conventional aluminosilicates. This innovative approach seeks to address challenges inherent in traditional geopolymer activation methods while contributing to environmental sustainability by reducing reliance on virgin raw materials and alleviating the accumulation of CDW. This study examines the performance of the geopolymer grout through a comprehensive series of experiments designed to assess the effects of mechanochemical activation on material properties. Specifically, the research evaluates the impact of WBP substitution on critical parameters, including fresh properties (e.g., flowability, setting time), mechanical performance (e.g., unconfined compressive strength (UCS), stress–strain behavior, bulk density), and microstructural characteristics (e.g., X-ray diffraction [XRD] and scanning electron microscopy [SEM]). Additionally, the role of GGBS as a partial replacement for WBP is analyzed to explore its synergistic effects on material properties and overall performance. The novelty of this research lies in the integration of recycled WBP into geopolymeric systems using mechanochemical activation, providing a cost-effective and eco-friendly alternative for construction applications. By advancing knowledge in this area, the study contributes to sustainable construction practices and addresses critical knowledge gaps in developing and applying innovative geopolymer technologies.

2. Experimental program

2.1 Materials

In this study, WBP and GGBS were employed as sources of aluminosilicate materials for producing geopolymer grouts, both mechanochemical and conventional (Figure 1). Grinding WB collected from different demolition sites around Baghdad and made in different factories in northern Iraq was used to produce WBP. The GGBS was retrieved from an Iraqi steel plant located in Basra. Using a Mastersizer 2000, the laser diffraction technique was used to determine the materials' particle size distribution (Figure 2). The physical and chemical characteristics of aluminosilicate materials' sources are displayed in Table 1. The WBP and GGBS had median particle sizes (d50) of 42.25 and 21.6 µm, respectively. The WBP and GGBS have specific surface areas of 0.72 and 1.46 m^2/g, respectively. The combination of silicon, aluminum, and iron oxides in the WBP, as indicated in Table 1, is greater than 70%, indicating that these materials meet the ASTM C618 criteria for pozzolanic materials. The energy-dispersive spectroscopy (EDS) micrographs correspond to the peaks of aluminum, silicon, and oxygen (Figure 3). This observation aligns with the data of X-ray fluorescence (XRF) spectroscopy shown in Table 1 and the reported EDS findings of Mahmoodi et al. [36].

(a) (b)

Figure 1. Waste sources of aluminosilicates. (a) WBP and (b) GGBS.

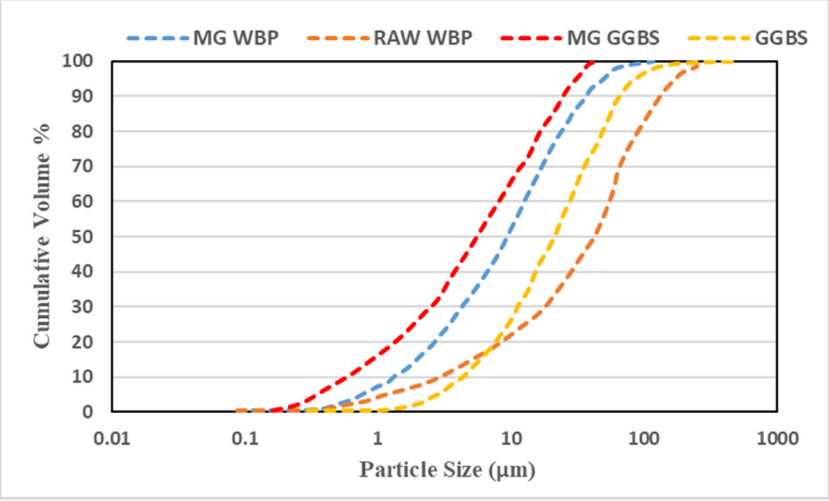

Figure 2. Particle size distribution of grout materials.

Constituent (%)	GGBS	WBP	(Na_2SiO_3-Penta) powder	(Na_2SiO_3) liquid
	(a) Chemical composition			
CaO	34.15	9.8		
SiO_2	40.42	55.5	28	29.4
Al_2O_3	10.6	17		
Fe_2O_3	1.28	5.5		
MgO	7.63	2.6		
SO_3	0.68	1.92		
K_2O	0.0128	1.58		
Na_2O	0.64	0.65	29	14.7
Modulus ratio			1	2
H_2O			43	55.9
	(b) Physical properties			
Specific surface area (m^2/g)	1.46	0.72		
D_{50} (μm)	21.6	42.25		

Table 1. Properties of WBP, GGBS, and sodium silicate.

However, the poor reactivity and minimal strength gain of WBP when cured at room temperature limits its wider usage in geopolymer synthesis [21]. Since GGBS has considerable mechanical strength and strong endurance in corrosive settings, it is added to the WBP-based geopolymer grout to address the low reactivity of the WBP employed in this work [37]. However, the GGBS binder has several undesirable characteristics, including high viscosity, quick setting, poor workability, and significant shrinkage [38–42]. According to past research, when the GGBS and WBP are combined in synthesis geopolymer mixes, they exhibit superior compressive strength, less shrinkage, and increased reactivity compared to their respective sole utilization [43,44].

This investigation selected sodium silicate and NaOH as the alkaline activators. A sodium hydroxide solution with a molarity of 5 M was prepared one day prior to mixing. This solution was synthesized by dissolving locally sourced NaOH beads (97–98% purity) in faucet water. Two kinds of sodium silicate (Na_2SiO_3) were utilized: a liquid solution for the conventional geopolymer and a powder form (sodium metasilicate-Penta) for the mechanochemical geopolymer.

To manufacture the alkaline activator, a ratio of Na_2SiO_3/NaOH = 1 was chosen based on past publications that used the mechanochemical activation technique [45]. The chemical and physical characteristics of sodium silicate in both liquid and powder forms, as well as the precursor components (WBP and GGBS), are shown in Table 1.

2.2 Geopolymer preparation

Mechanochemical activation was used in this study to create geopolymer grouts in contrast to traditional activation. According to Hamid Abed et al. [46], the raw material powders (NaOH, sodium metasilicate, WBP, and/or GGBS) had to be ground for 2 h in order to prepare the MG precursor (Figure 4). A ball mill with 10 kg capacity was used for the grinding process utilizing a 3:1 ratio (3 kg ball/1 kg solid material), with different ball sizes (15–40 mm) to get a high-performance grinding process according to Raghuraman et al. [47].

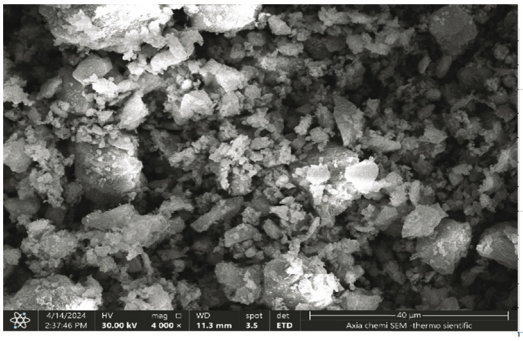

Element	Wt %	σ
C	17.0	0.3
O	40.7	0.6
Na	0.5	0.1
Mg	2.5	0.1
Al	5.4	0.1
Si	18.0	0.1
K	1.0	0.0
Ca	10.3	0.1
Ti	0.5	0.0
Fe	4.1	0.1

Figure 3. EDS analysis of WBP powders.

Due to the constant impact of the grinding and particles, the mixed raw materials' components (particles) become trapped between the balls and the container wall during the ball milling (grinding) process. The MG precursor resulting from the milling was added with tap water to create an MG grout, as prescribed by Abbas et al., and Hamid Abed et al. [13,14,46].

The conventionally activated geopolymer was substituted in formulating the conventionally activated geopolymer (CG)-grout with the MG technique to enable comparisons. The distinct impacts of the two activation techniques on the geopolymer grout preparations can be determined via this substitution. NaOH beads were dissolved in tap water at a molarity of 5 for standard geopolymer preparations, and their weight was subsequently recorded. According to Ilcan et al. [48], 5 M NaOH was identified as the optimal choice, balancing early strength development, workability, cost-effectiveness, and minimizing potential environmental impacts associated with high alkalinity, which may lead to increased cost and potential efflorescence without significant performance enhancement. It is important to note that the mixing procedure produced an exothermic reaction, which caused the NaOH solution to heat up considerably. Before being used again, the liquid was left to cool at room temperature of 23 ± 3°C for 24 h and stored until chemical equilibrium was reached. The cooled NaOH liquid was then mixed with sodium silicate (Na_2SiO_3) in accordance with the standard geopolymer activation protocol. This was cautiously done to minimize any danger related to the exothermic reaction and to guarantee secure handling of the extremely alkaline NaOH solution.

This study utilized two mixture groups (MG and CG). In each mixture group, the WBP was replaced by GGBS in ratios of 0, 15, 30, and 45%. For instance, the CG-0S-100B code indicates that the adopted grout was a CG with 0% GGBS and 100% WBP. The MG-45S-55 WBP code indicated a mechanochemically activated geopolymer grout with 45% GGBS and 55% WBP. The MG and CG mixture ratios are shown in Table 2. The 15–45% range for WBP replacement was chosen to balance the performance and sustainability

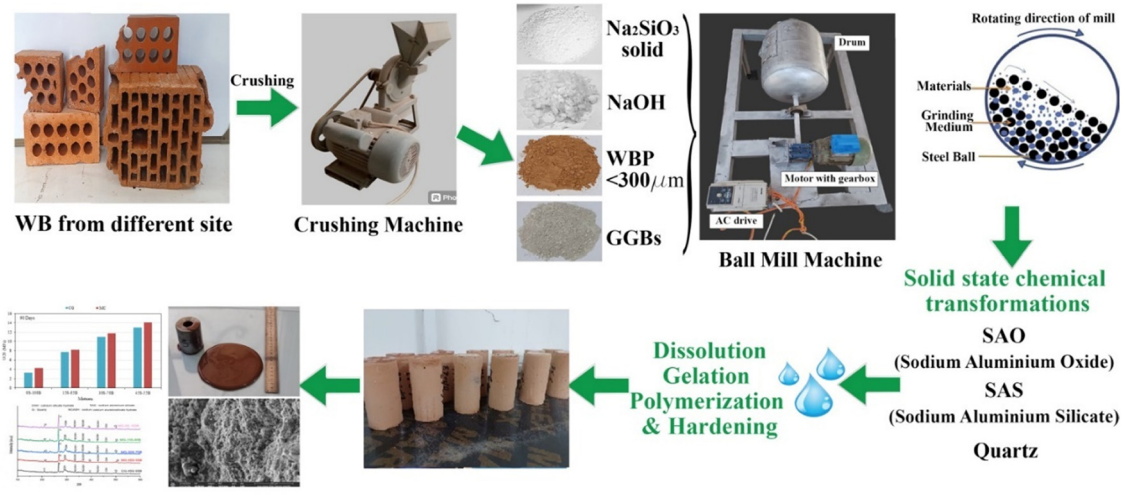

Figure 4. Process of producing a geopolymer binder through mechanochemical activation.

goals. This range allows for significant waste utilization while maintaining adequate mechanical properties in the geopolymer grout, aligning with findings from previous research on geopolymers with waste materials [49].

2.3 Testing methods

All the prepared specimens were created in the lab at 23 ± 3°C (room temperature). The mini-slump flow test was used to investigate the geopolymer grout's fresh properties in compliance with Kantro and Güllü and Ali Agha [50,51]. Using a small cone with dimensions of 19 mm for the top diameter, 38.1 mm for the lower diameter, and 57.2 mm for height, the slump flow test was used to determine the grout's spread diameter (measured in millimeters). The average of two measurements in two perpendicular directions resulted in the final grout spread diameter. The Vicat needle penetration tests were carried out to ascertain the grout mixtures' setting timeframes in accordance with ASTM C191-19 [52]. Only the final setting time results were taken into consideration for discussion in this study.

Regarding mechanical characteristics, the grout mixes were poured into cylindrical molds of 50 mm in diameter and 100 mm in height. The samples were allowed to cure for 28 and 90 days at 23 ± 3°C. Then, standards were used to measure the grout samples' UCS [53,54]. Mechanical testing was conducted on three specimens per mixture, and the average strength was determined. It is important to mention that before conducting the UCS testing, the samples were used to measure the bulk density of the hardened geopolymer grout. A Thermos Scientific Axia device model was utilized to conduct SEM examination on raw GGBS and WBP powders and on co-ground GGBS and WBP with solid chemicals. This was carried out to look into the microstructure alterations brought on by the mechanochemical activation process. Furthermore, SEM analysis was carried out on the hardened geopolymer grouts (MG and CG) in order to evaluate the impact of GGBS/WBP substitution and the activation procedure. The specimens tested under UCS were used to obtain samples for SEM evaluation. These samples were taken from fractured particles and were then coated with gold to ensure accurate SEM imaging. The diameter and height of the samples were roughly 20 and 10 mm, respectively. Additionally, the chemical composition of the WBP powder was ascertained using an energy dispersive spectrometer. Furthermore, XRD was used to qualitatively evaluate each geopolymer precursor's crystalline structure pre- and post-mechanochemical activation on top of examining the impact of the GGBS/WBP substitution. The potential for heavy metal

Table 2. Mixing proportions of CG- and MG-based grouts.

		Weight (%)					Weight (g)							
		Aluminosilicate materials		Alkaline activator		Na_2SiO_3/NaOH	Aluminosilicate materials		Alkaline activator		w/b ratio	Ball-Mill duration (h)	NaOH molarity
Activation type	Mix ID	WBP	GGBSF	NaOH	Na_2SiO_3		WBP	GGBSF	NaOH	Na_2SiO_3			
MG	MG-0S-100B	80	0	10	10	1	800	0	100	100	500	**2**	5
	MG-15S-85B	68	12	10	10	1	680	120	100	100	500		
	MG-30S-70B	56	24	10	10	1	560	240	100	100	500		
	MG-45S-55B	44	36	10	10	1	440	360	100	100	500		
CG	CG-0S-100B	80	0	10	10	1	800	0	100	100	500	—	5
	CG-15S-85B	68	12	10	10	1	680	120	100	100	500	—	
	CG-30S-70B	56	24	10	10	1	560	240	100	100	500	—	
	CG-45S-55B	44	36	10	10	1	440	360	100	100	500	—	

leaching from grout at geotechnical application in contact with subsurface water was evaluated using the toxicity characteristic leaching procedure (TCLP) outlined in the EPA Method 1311 [55]. This assessment focused on WBP, GGBS, and a high-strength geopolymer grout specimen. Following size reduction to <9.5 mm, a 10 g sample was immersed in 200 mL of acetic acid solution (pH 2.9), maintaining a 20:1 liquid-to-solid ratio. The mixture was agitated for 18 h at 20°C and 30 rpm, followed by filtration through a 0.7 µm glass fiber filter. Leached heavy metal concentrations in the filtrate were subsequently quantified via inductively coupled plasma-atomic emission spectrometry (ICP-AES).

3. Results and discussion

3.1 Microstructure analysis of solid geopolymer precursors

The microstructure of the raw and mechanochemically ground GGBS and WBP precursors was examined using SEM. It is evident from Figure 5(a) that the raw WBP had an angular porous surface and an irregular shape. The GGBS components also show sub-rounded to angular forms, and the material particles were heterogeneous and different, as shown in Figure 5(b). The edges and roughness were observable in angular particles and bulk (Figure 5) [56].

The solid chemical powder (a mixture of sodium silicate and NaOH) was used to coat the WBP particles after they had been ground using sodium metasilicate and NaOH. This resulted in a decrease in the WBP's solid chemicals and average size. As a result, the geopolymeric precursor was formed. Furthermore, the combination of NaOH and sodium metasilicate led to the first binding between the WBP particles, as shown in Figure 6(a). Furthermore, Gupta et al. [18] observed that after 8 h of ball-milling fly ash and NaOH, cracks and flaws developed, increasing the surface area and enhancing the reaction. As shown in Figure 6(d), it is clear that the size of the GGBS particles reduced typically when they were added to the WBP-based MG precursor system, although they still have angular and deformed morphologies. Additionally, the 2-h mechanochemical procedure enhanced the particles' surface area and accelerated the geopolymer precursors' reaction rate [14].

Figure 7 presents the XRD patterns of raw WBP and a WBP-based MG precursor. The analysis shows that the raw WBP has a significant vitreous phase itemized from the halo around $2\theta = 18°–20°$ and significant crystalline quartz phases based on the sharp peaks recorded between $2\theta = 20°$ and $2\theta = 70°$. Similarly, Hwang et al. [57] demonstrated the mineralogical composition of the WBP using XRD, revealing that quartz is the predominant crystalline phase in the WBP. The diffractogram of the WBP-based MG denotes a significant amorphous phase on top of a decrease in the peak intensity corresponding to crystalline phases. Additionally, phases such as sodium aluminosilicate were observed. When comparing the WBP-MG precursor to raw WBP, the comparative study of the XRD patterns in Figure 7 shows the emergence of new peaks like sodium aluminosilicate and the elimination of other crystalline phase peaks. The loss of crystalline phases confirms the amorphization

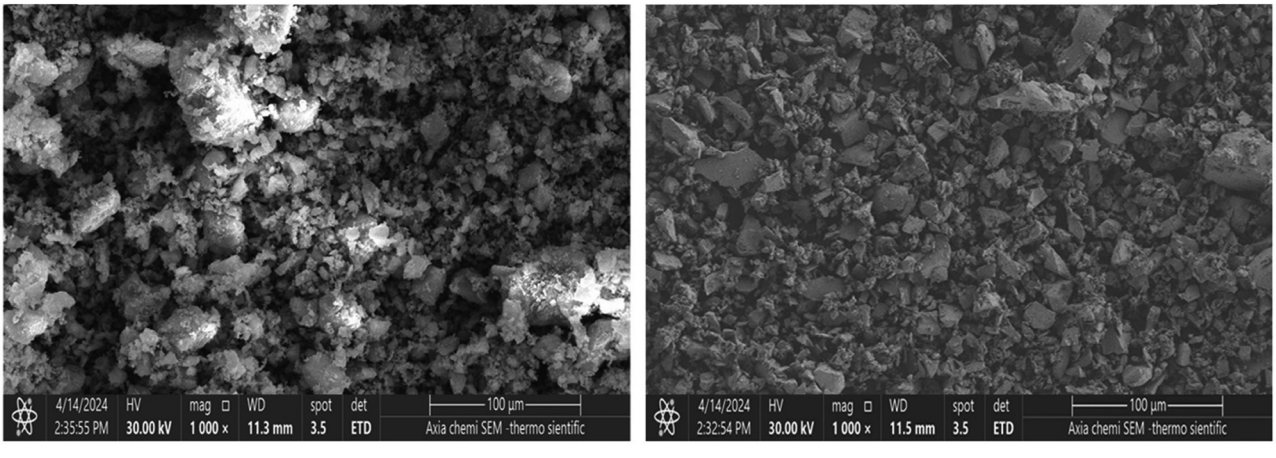

Figure 5. SEM images of (a) raw WBP and (b) raw GGBS.

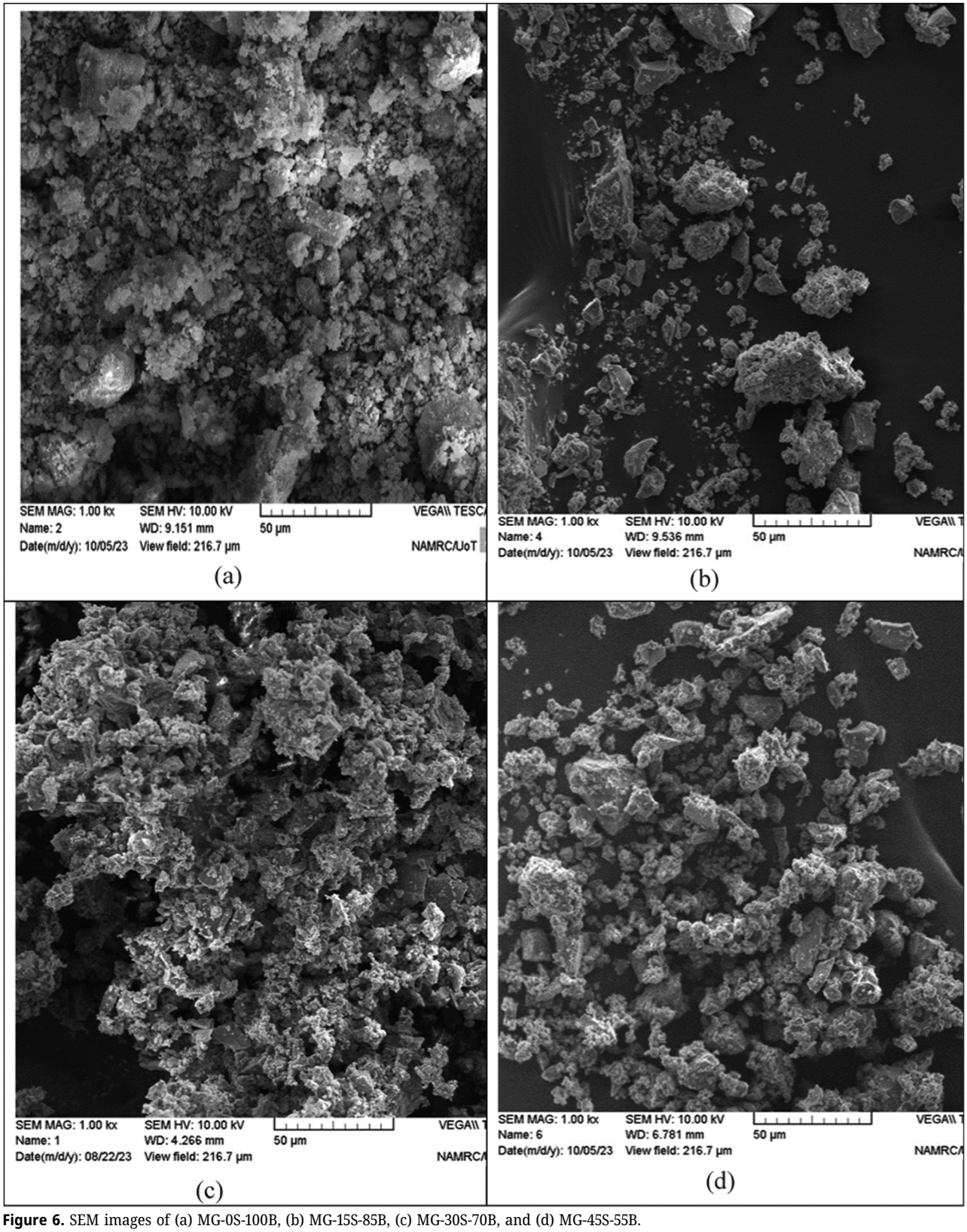

Figure 6. SEM images of (a) MG-0S-100B, (b) MG-15S-85B, (c) MG-30S-70B, and (d) MG-45S-55B.

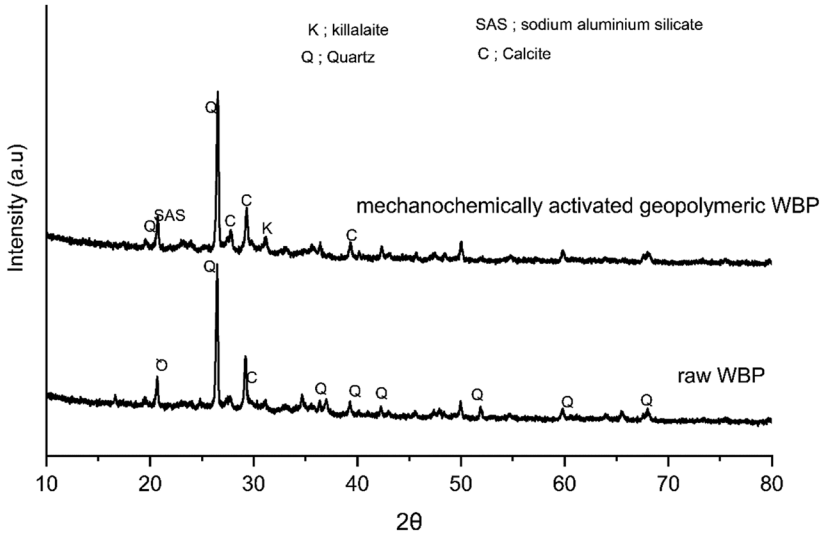

Figure 7. XRD patterns of raw WBP and WBP-based MG precursor.

upon grinding, and the synthesis of new material is confirmed by the presence of new phases (i.e., the WBP-MG precursor). A comparable observation was made by Hamid Abed et al. [58] and Hosseini et al. [17] who recorded a more diminished peak intensity of the geopolymer precursor activated mechanochemically. This attenuated peak intensity indicates an additional breakdown of the crystalline structures of the quartz and alumina phases, as well as modifications in the crystalline structure subsequent to grinding.

Figure 8 depicts the effect of GGBS substitution on the mineralogical compositions of the WBP-based MG precursor. The quartz peaks' intensity lessened substantially as the content of the GGBS spiked in the WBP-based MG precursor. The samples with 100% WBP (MG-0S100B) showed the highest peaks of the WBP-MG precursor samples. The MG-0S100B mixture was analyzed to determine whether any crystalline species in WBP participate in the mechanochemically activated geopolymerization process. The higher-intensity quartz peaks in the MG-0S-100B precursor verify a lower degree of geopolymerization than in the WBP-MG precursor including GGBS. The varied crystalline quartz intensity peaks indicate varying extents of geopolymerization in the precursor. The faster rate of the mechanochemically activated geopolymerization reaction

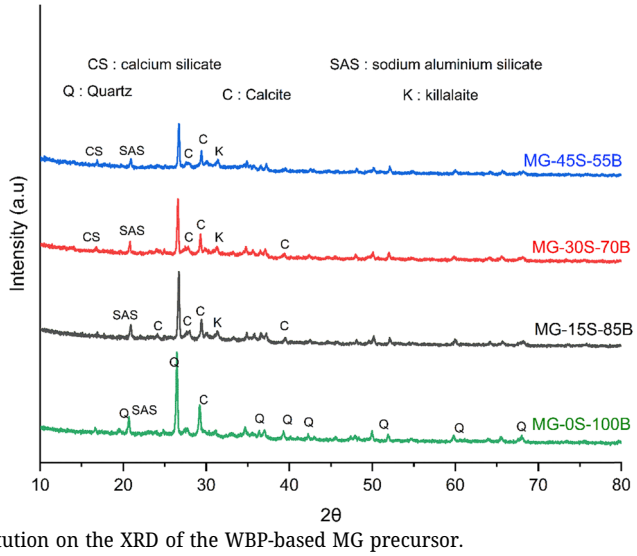

Figure 8. Effect of GGBS substitution on the XRD of the WBP-based MG precursor.

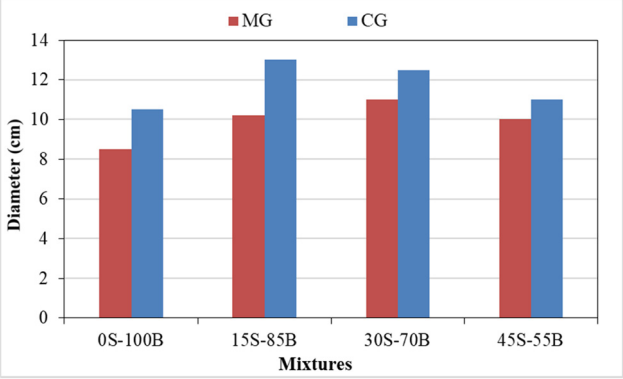

Figure 9. Workability of mechanochemical and conventional activation of mixtures.

was caused by the higher GGBS content, while the MG-45S-55B mixes displayed the lowest quartz peak intensity. The higher rate reaction will remarkably enhance the compressive strength [45]. It is clear that new semicrystalline mineral phases were added to the MG precursor by the reaction of the WBP-MG precursor with GGBS.

3.2 Fresh properties

3.2.1 Flowability test

Figure 9 displays the MG and CG mixtures' flowability test with different GGBS/WBP ratios. The slump flow values of MG and CG were measured in the ranges of 85–110 mm and 105–130 mm, respectively. The reference mixtures (MG-0S-100B and CG-0S-100B) comprising 100% WBP exhibited the lowest slump flow values. The diminished flowability observed in the WBP bead geopolymer grout can be attributed to the porous surface of the unreacted brick waste. This surface readily absorbs water from the fresh mixture, thereby reducing the free water content within the mixture [59,60]. Additionally, the irregular shape of BP particles may further contribute to the compromised workability of the geopolymer [23,57]. A similar observation was made by Hwang et al. [57], who noted that alkali-activated paste mixes containing solely WBP exhibited the lowest slump flow values, which were enhanced by incorporating GGBS. As shown in Figure 9, the increase in the GGBS content significantly affects the results of the flowability of all the mixtures regardless of the geopolymer type. The mixtures MG-15S-85B, MG-30S-70B, and MG-45S-55B exhibited slump flow values that are 20, 29, and 18% higher, respectively, compared to the reference mixture MG-0S-100B, which comprised 100% WBP. Conversely, CG-0S-100B displayed slump flow values that are 24, 10, and 5% lower than those of CG-15S-85B, CG-30S-70B, and CG-45S55B, respectively. In both sets of mixes, a discernible upward trend in slump flow was observed with an increase in the proportion of GGBS until reaching 15 and 30% of GGBS content. Subsequently, a downward trend in slump flow was observed with further increases in the proportion of GGBS beyond 45%, as depicted in Figure 9. The porous surface of the unreacted WBP may be the cause of the mixture's decreased workability at high WBP contents [61]. On the other hand, the results demonstrated the effect of the activation method (mechanochemical activation) on the geopolymer grout's slump flow. Hence, the MG grout samples' slump flow decreased by 10–27% compared to CG grout samples (Figure 9). This could be related to the powder's altered surface area and particle size due to mechanochemical processing, indicating that more water is required to cover the particles' surface. This causes a noticeable increase in apparent viscosity and lower flowability in fresh grouts and a notable decrease in free water [13,14]. Reduced slump flow necessitates adjustments in injection pressure or mix design to ensure proper penetration in confined spaces [46]. Moreover, a range of 10–20 cm for slump flow is often suitable for most grouting applications, ensuring adequate flowability and penetration (ASTM C1437) [62]. However, the desired slump flow may vary depending on the grout type, void geometry, and injection pressure. A comprehensive assessment of project requirements and site conditions is crucial for determining the optimal range. Meanwhile, Hamid Abed et al. [14,63–65] observed that mechanochemical activation induced the fragmentation of large aluminosilicate particles into smaller constituents, thereby amplifying the surface area and fostering a more homogeneous distribution of alumina derived from slag and fly ash. Consequently, this phenomenon precipitated a noteworthy decline in free water content within fresh grouts, accompanied by a conspicuous elevation in apparent viscosity.

3.2.2 Final setting times

Setting time is a critical parameter in grouting applications, whereby a short setting time could impair the grouting equipment, while a long setting time typically slows down the construction timeline [13]. Figure 10 illustrates the effect of the WBR/GGBS ratio on the MG and CG grouts' setting times. The results demonstrated that the mixtures containing 100% WBP had the longest final setting times, spanning 235 and 260 min for MG and CG, respectively. Meanwhile, it is noteworthy that the GGBS content plays a significant role in determining the setting time of WRP-based geopolymers, with the higher GGBS content showing a considerable decrease in setting time. However, as the GGBS content increased to 15, 30, and 45%, the final setting time decreased to 132, 110, and 90 min, respectively. Setting time determines the working time available for placement, with shorter setting times necessitating faster injection or smaller batches [13,66]. Generally, a setting time between 1 and 4 h allows for sufficient workability while preventing premature hardening (ACI 224R-01) [67]. The desired setting time may vary based on the project scale, injection method, ambient temperature, and need for adjustments. The decrease in setting time with increasing GGBS content can be ascribed to the higher reactivity exhibited by GGBS compared to WRP [24]. Furthermore, the hastened setting process may be attributed to the increased dissolution of Ca^{2+} ions from GGBS [68,69]. According to Migunthanna et al. [21] and Hamid Abed et al. [63,64] higher GGBS contents contribute to an increased presence of CaO in the reaction medium. This CaO dissolves faster than silica and alumina, providing additional nucleation sites that facilitate a faster setting time for WBP-based geopolymers. This heightened dissolution results in the release of significant hydration heat, forming calcium silicate hydrate (C–S–H) or C–A–S–H gels, consequently accelerating the polymerization process [70]. It is pertinent to note that incorporating an excessive proportion of GGBS in WBP-based geopolymers has led to an acceleration in the setting time. However, this shortened setting duration may pose a potential risk to the grouting machinery. The rapid setting process could impose excessive pressure or strain on the equipment, increasing the likelihood of wear and tear or equipment failure. Furthermore, the accelerated setting process may compromise the workability of the geopolymers, adversely affecting their usability. Consequently, it is imperative to meticulously regulate the GGBS ratio in WBP-based geopolymers to achieve the optimal setting time and workability while ensuring the maintenance of desired quality and performance standards.

Figure 10 presents the final setting time of the WBR/GGBS-based geopolymer as an effect of the activation method. The experimental results indicate a notable impact of mechanochemical activation on the setting time properties of geopolymer grout; the final setting time of MG-0S-100B, MG-15S85B, MG-30S70B, and MG-45S55B mixtures exhibited reductions of 11, 25, 14, and 9%, respectively, compared to the corresponding setting times of CG grout, as depicted in Figure 8. The shortened setting time observed in MG grout may be ascribed to the mechanochemical activation process, which induces an increase in the surface area and a reduction in particle size. This phenomenon exposes a larger surface area to chemical reactions [20,71]. Consequently, these conditions facilitate enhanced particle dissolution, geopolymerization, and reaction rates, thereby promoting the adsorption of free-mixing water and ultimately reducing the setting time in MG grout. According to Hamid Abed et al. [46], mechanochemical activation leads to a higher proportion of evenly distributed alumina derived from GGBS and fly ash, thereby enhancing its participating and dissolving ability for geopolymer gel formation. Large aluminosilicate particles breaking up into smaller ones are thought to be the cause, which increases the

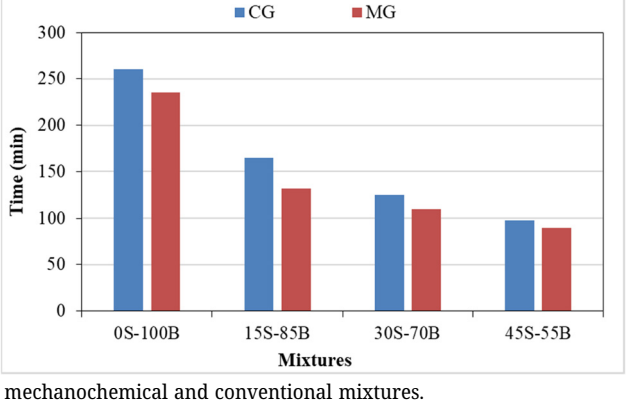

Figure 10. Final setting times of mechanochemical and conventional mixtures.

mixture's surface area and uniformly distributes the particles [72,73]. The heightened availability of aluminosilicates accelerates the geopolymerization reaction, consequently contributing to a shorter setting time for MG grout.

3.3 Mechanical properties

The UCS of the geopolymer mixtures with various WBP/GGBS ratios are presented in Figure 11. The UCS tests were performed at two different geopolymer paste ages namely, 28 and 90 days. It was observed that the UCS values of all the mixtures exhibited improvement as the age progressed from 28 to 90 days. This enhancement can be attributed to the completion of the geopolymerization process and densification of the microstructure occurring at longer ages [74–76]. The lowest 28-day UCS (3–2 MPa) was achieved for the mixture where only WBP powder was used as the aluminosilicate precursor. As reported in Fořt et al. [77], since pure WBP was unable to set and harden, GBFS had to be added to get a more effective mixture. It was discovered that adding more CaO to the GBFS/WBP mixture resulted in a denser structure of the C–A–S–H gel, improving its strength [57]. Figure 11 demonstrates that substituting the WBP powder with GGBS resulted in a linear enhancement in strength and an increase in the GGBS level. The UCS values of the geopolymer mix demonstrated increases of 90, 174, and 227% when the WBP was substituted with 15, 30, and 45% GGBS, respectively, at 90 days. The noteworthy influence of GGBS on the UCS may be attributed to its superior cementing properties and increased reactivity in contrast to WBP. An important factor in boosting the activation process and early age strength is the high CaO content [78]. Moreover, the high CaO content may result in C–S–H/CA–S–H gels, changing the geopolymer grout mixture's microstructure and improving its mechanical qualities even more [79]. Additionally, the geopolymer grout's microstructure would compress and its porosity would decrease as a result of the production of C–A–S–H gels. Likewise, Hwang et al. [57] evaluated the effect of GGBS content on the strength properties of the alkali-activated BP. Previously, Sharmin et al. and Ahmed et al. [22,61] observed that the strengths increased with increasing GGBS content, which is consistent with the findings of the present investigation.

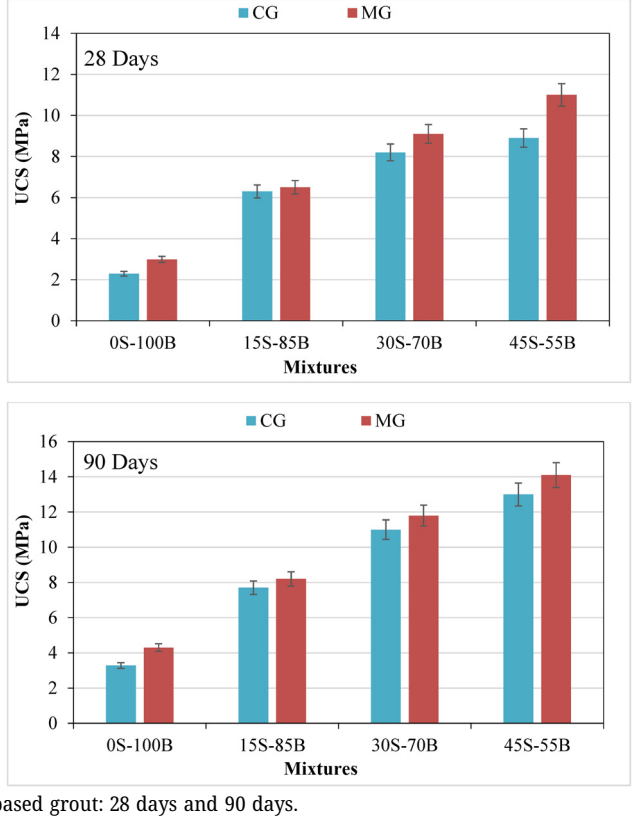

Figure 11. UCS of MG- and CG-based grout: 28 days and 90 days.

As demonstrated in Figure 11, the strength properties of the geopolymer samples are significantly impacted by the activation process (mechanochemical activation). After 90 days, the UCS of the MG samples revealed a strength enhancement of roughly 7–30% compared to the CG samples' counterparts (Figure 11). GGBS and WBP exhibited enhanced surface area and reactivity upon mechanochemical activation. More cementitious gel was formed as the primary reaction product resulting from the source materials' reactivity, and this gel formation filled the pore system. Better immobilization resulted from decreased porosity and reduced total pore volume of the geopolymer grout, which are caused by a greater amount of gel forming in the grout [46]. The material's resistance to external effects is determined by the movement of ions, water, and pore structure [80]. Additionally, the diffusion process during leaching is dependent upon the distribution of the pore size [81], the matrix's stability [82], physical properties [83], and microstructural characteristics, such as tortuosity and porosity [84]. Similar MG grout behavior was noted in the studies of Hamid Abed et al. and Hamid et al. [14,85], where it was shown that the mechanochemical activation procedure increased the geopolymer binders' surface area and reactivity. The end consequence of this was the creation of more gel inside the geopolymer matrix, which decreased the porosity and overall pore volume. As a result, this improved the particles' binding and increased the MG sample's strength.

It is important to mention that the CG grout with 45% GGBS (CG-45S-55B) samples exhibited surface cracks compared to the MG grout with the same ratio (Figure 12). More noticeable shrinkage was primarily responsible for the crack development in CG samples with 45% GGBS concentration [46]. According to Fořt et al. [77], compared to GGBS, the BP's increased crystalline content may result in less drying shrinkage and more flexural strength preservation.

The results of the stress–strain diagram of the CG and MG at different WBP/GGBS ratios are displayed in Figure 13. The stress–strain diagram of geopolymers with different WBP/GGBS ratios clearly displays substantial shape differences; mixtures with a low UCS had wide stress–strain curves, while the high UCS mixtures showed narrow stress–strain curves. It is possible to deduce that the strain properties of the mixtures are related to the way these curves behave. Stated differently, a significant relationship exists between the initial UCS and strain. Samples with higher initial UCS showed less strain than those with lower initial UCS. The stress–strain behavior of the MG grout regardless of the replacement level of WBP is not much different than that of the typical CG grout. In other words, the influence of the activation method of the geopolymer grout on the stress–strain behavior is minor. The replacement of GGBS with WBP resulted in reducing the stress of the geopolymer grout. The geopolymer grouts' stress decreased with increasing amount of WBP due to the low amount of CaO in BP and due to the important role of calcium dioxide in the activation process and early age strength of the geopolymer grout [78]. The experimental results show the significant impact of the WBP on the geopolymer grouts' strain behavior, whereby the MG strain increased from 0.015 to 0.024, and the strain capacity of

Figure 12. Surface images of MG- and CG-based grouts.

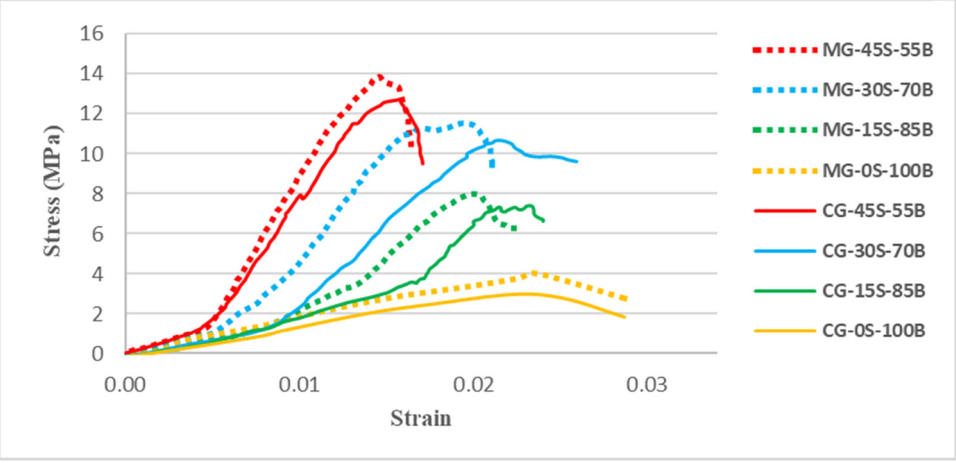

Figure 13. Stress–strain responses of mixtures.

CG increased from 0.016 to 0.024 when the GGBS amount was replaced with 55% of WBP. In other words, the strain capacity of MG increased by 60% when the amount of GGBS was fully replaced with WBP. BP can weaken the chemical binding and strengthen the frictional bond, which increase the strain capacity of the geopolymer grout. This increases the strain observed by including WBP powder in both the MG and CG grouts [61]. According to Ahmed et al. [61] and Wang et al. [86], the inclusion of WBP improves the flexibility of strain-hardening cementitious composites, which increases the final displacement of these materials along with the increase in the replacement of WBP.

For the validation of UCS results, a bulk density test was conducted for both MG and CG grouts, as displayed in Figure 14. It is evident that the density results followed the same trend as observed for UCS, with a minimum of 1,762 kg/m^3 for the pure WBP-based geopolymer and a maximum of 1,875 kg/m^3 for the geopolymer with 45% GGBS content after 90 days of curing. It is apparent that the density values exhibited a gradual increase as the GGBS content increased. Through the alkali activation reaction, more C–S–H and C–A–S–H gels gradually formed due to the greater CaO content and amorphous character of GGBS [57]. The hardened paste's porosity is subsequently reduced as a result of the creation of these extra gels, which is necessary for the formation of a denser morphology. This denser morphology ultimately results in increased strength and density for the geopolymer grout samples [46]. The results showed that the MG samples had a 3% higher density than the CG grout samples (Figure 14). The geopolymer grout's increased surface area and reactivity resulted from the ball-milling of GGBS/WBP and chemical powder (NaOH and sodium metasilicate), which is responsible for the higher density of the MG samples. Because of the improved reactivity of the source materials, more gel was formed as the primary reaction

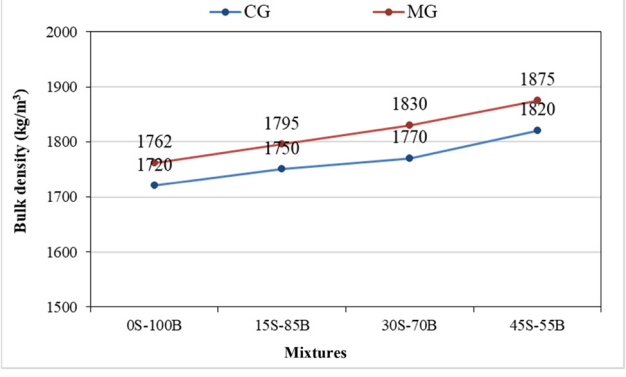

Figure 14. Bulk density of MG- and CG-based grouts.

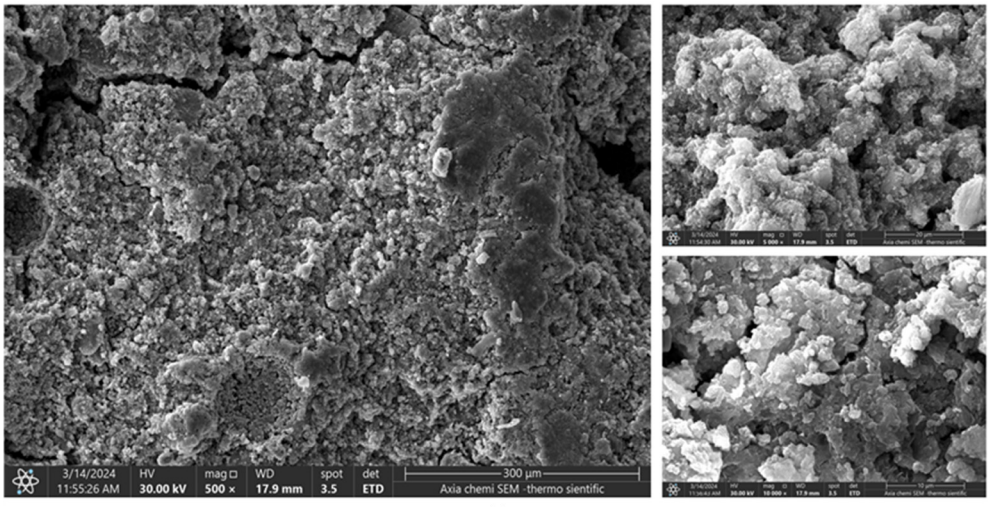

(a)

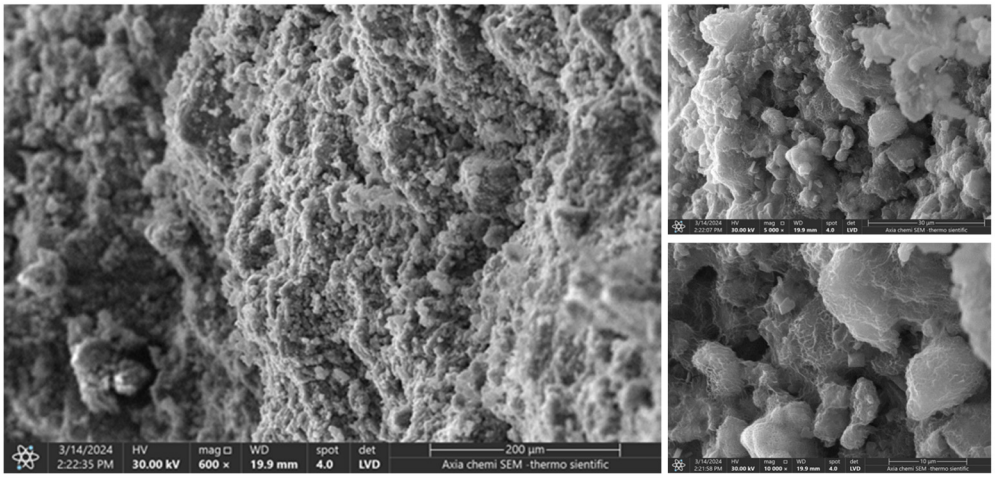

(b)

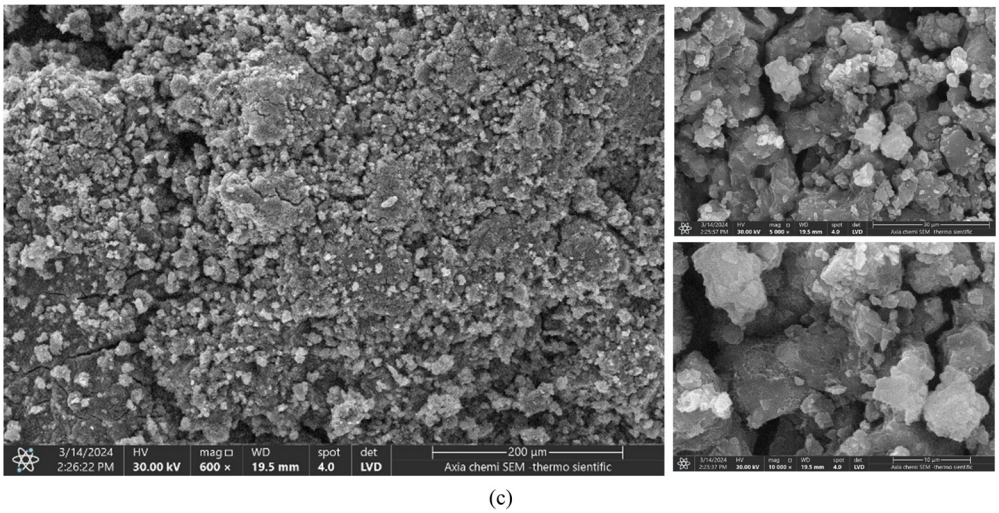

(c)

Figure 15. SEM images of the (a–e) hardened grouts ((a, b, c, d) MG and (e) CG). (a) MG-0S-100B, (b) MG-30S-70B, (c) MG-15S-85B, (d) MG-45S-55B, and (e) CG-45S-55B.

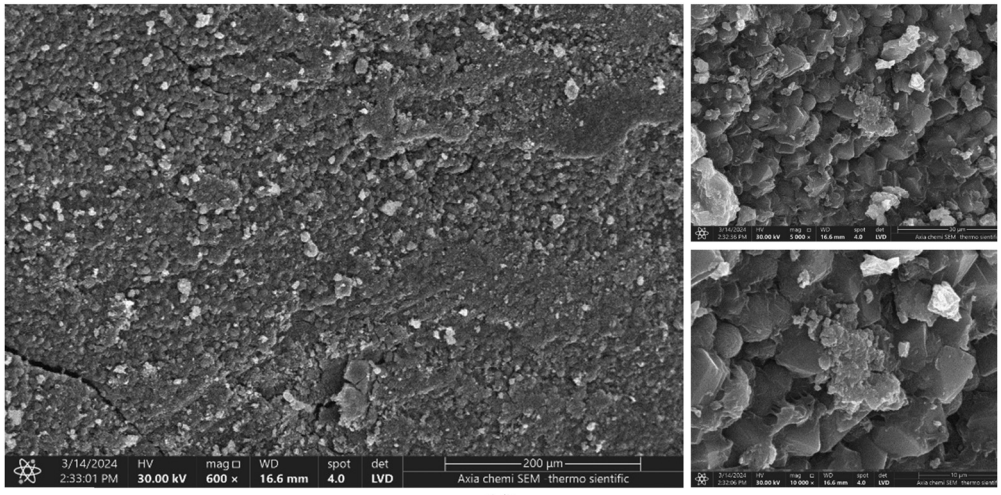

(d)

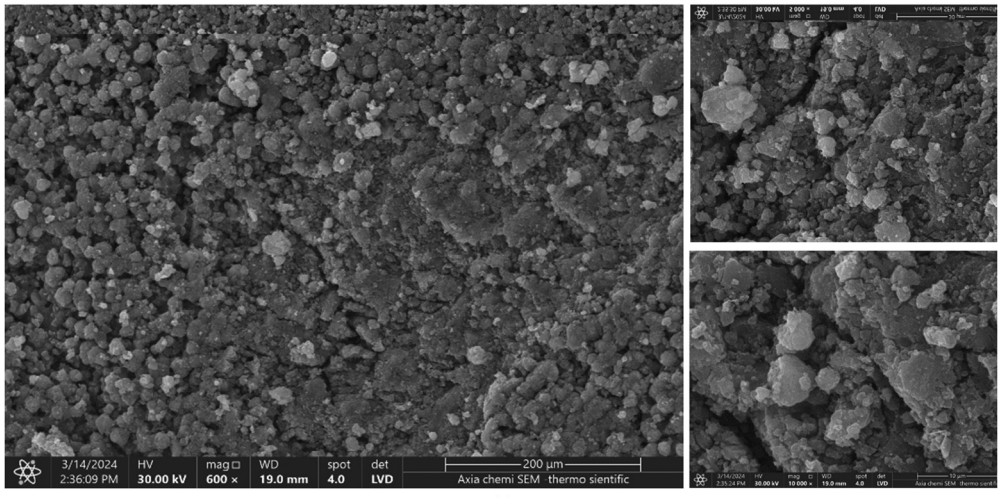

(e)

Figure 15. (*Continued*)

product, which decreased the porosity and increased the MG grout's density [14].

3.4 Microstructural analysis of geopolymer grouts

The impact of GGBS substitution and activation method on the microstructure of the WBP-based geopolymer grout is shown in Figure 15. The microstructure characteristics of the WBP-based geopolymer grout were considerably impacted by the increased GGBS concentration, as demonstrated by the SEM images. There was a noticeable difference in the blends with 0, 15, 30, and 45% GGBS. The microstructure features of the pure WBP-based geopolymer grout showed a loose and fragmented morphology, as shown in Figure 15(a). Similarly, Fořt et al. [44] noted that the reaction rate of geopolymer mixes with WBP decreased, leading to a less compact microstructure and the presence of unreacted particles. Furthermore, the system contained an amount of partially or completely non-reacting particles. When 15 and 30% of GGBS were added to the WBP, the particles of the MG grout samples became even more compact and homogenous, as shown in SEM images in Figure 15(b) and (c). The development of C–S–H and C–A–S–H on top of the hydrated N–A–S–H gel was aided by the Ca^{2+} from GGBS entering the Si–O–Al–O structure of the WBP-based geopolymer grout system as the amount of GGBS in the system increased. The said finding is consistent with that of Ismail et al. [87].

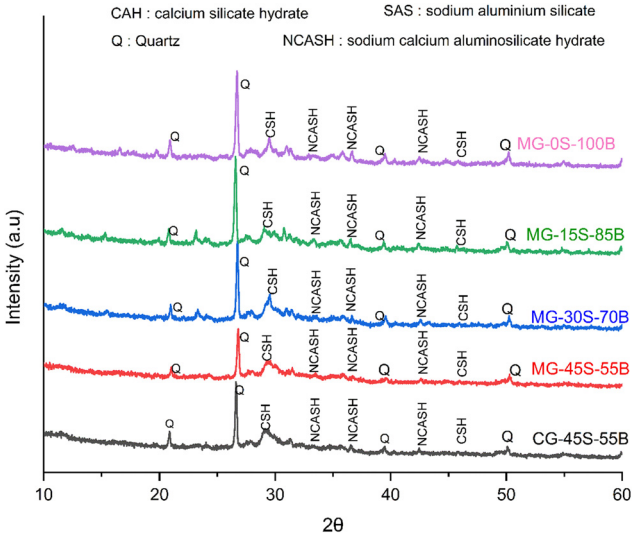

Figure 16. XRD patterns of CG- and MG-based grout samples.

It was observed that the geopolymer samples with 45% GGBS were more structurally compact and homogeneous with produced gels and had fewer particles with no reactive contribution, as shown in Figure 15(d), compared to the counterpart samples with 100% WBP, as shown in Figure 15(a), that were more microstructurally porous and less cohesive. Conversely, the XRD test indicates that GGBS is amorphous, contributing to a higher alkali activation reaction rate and an intensified synthesis of C–S–H and C–A–S–H, both of which boosted strength [57].

The MG samples had a well-dispersed, compact morphology with partially reacted powders surrounding it, as shown in Figure 15(b) and (d). In contrast, the CG samples showed a less dense, fragmented morphology with a greater quantity of unreacted starting powders. Comparing the MG to the CG, Abbas et al. [13] found that the former's performance is denser and more compact. Compared to the MG samples, which seemed to be well-connected by a gel-like network, unreacted particles are more visible in the CG samples, producing a looser microstructure and less C–S–H gel. More gel was formed within the geopolymer-stabilizer matrix as a result of the mechanochemical activation process, which increased the geopolymer grout's surface area and reactivity [14,85]. This strengthened the bond between the particles and improved the microstructure characterization of the MG grout sample by lowering the total pore volume and porosity.

XRD was used to analyze the mineralogical compositions of the geopolymer grout samples in order to investigate the effects of the activation process and the GGBS substitution on the solidified geopolymer grout (Figure 16). It was demonstrated that the formation of new phases during the alkali-activation process is what led to the formation of the new semicrystalline phases. During the alkali activation process, some unreacted particles from the initial materials remained in their crystalline forms. Expectedly, quartz (SiO_2) was the major crystalline mineral found in all the geopolymer grout samples. In both the MG and CG grout samples, it remained as an unreacted particle, as evident from 2θ values of 20.85°, 27.3°, 39.9°, and 50.71° (ICDD# 05-0490). This result concurs with the previous research [57].

Sample name	Pb	Cd	Cr	Zn	Cu	Ni	As
EPA limit (mg/L)	**5**	**1**	**5**	**25**	**25**	**25**	**5**
MG-45S-55B (mg/L)	0.251	0.232	1.739	2.462	0.74	0.73	Not detected
CG-45S-55B (mg/L)	2.965	0.102	2.724	1.642	0.96	<0.01	Not detected
GGBS (mg/L)	<0.01	0.013	0.076	Not detected	0.025	0.02	<0.01
WBP (mg/L)	<0.01	0.019	0.672	1.246	0.5	1.697	<0.01

Table 3. Results of TCLP analysis.

However, the quartz peaks' intensity lessened substantially with the increase in GGBS content in the MG samples; hence, 100% WBP (MG-0S-100B) samples demonstrated the highest peaks for the MG grout samples. Meanwhile, the MG-45S-55B mixtures demonstrated the lowest intensity in the quartz peak, because the higher GGBS content results in a greater alkali activation reaction, adding the system with more gel. The gelation process lessens the unreacted WBP and creates a more compact system, thus enhancing the strength significantly [61]. The SEM images of the MG grout samples supported this finding. As reported by Hwang et al. [57], the WBP's reaction to the GGBS presented the geopolymer matrix with new semicrystalline mineral phases.

In terms of the activation method's impact, the MG grout samples showed significantly higher crystalline quartz intensities compared to the CG-based grout samples, as depicted in Figure 16. A similar observation was reported by Abed et al. and Hamid Abed et al. [45,63]. According to Hosseini et al. and Gupta et al. [17,18,88,89], the XRD patterns of the set CG and MG grout samples showed the presence of novel products and the crystal phase spikes found in the initial powder. These products, which are primarily made up of synchronized alkaline amorphous aluminosilicate gels, are essentially the outcome of alkali-activation processes. The primary peaks fit into the following categories: (1) calcium silicate hydrate (C–S–H) gel, both found in the CG and MG grouts (Figure 10) at 29.5° and 46.2° (ICDD# 03-0649) and (2) C–A–S–H and N–A–S–H gels coexisting as sodium calcium aluminosilicate hydrate (N–C–A–S–H) at 33.6°, 36.3°, and 41.5° (ICDD# 25-0777) both found in the CG and MG grouts. These findings are consistent with those of Zawrah et al. and Rovnaníková et al. [43,90].

3.5 TCLP results

To evaluate the potential environmental impact of solidified geopolymer grout samples (specifically, MG-45S-55B and CG-45S-55B) after a curing period of 28 days, the TCLP was conducted. This analysis, which was performed in accordance with the United States Environmental Protection Agency Method 1311, as detailed in Table 3, focused on assessing the leachability of seven key heavy metals: arsenic (As), cadmium (Cd), chromium (Cr), copper (Cu), nickel (Ni), lead (Pb), and zinc (Zn). From an environmental perspective, using recycled materials or solid inert waste in field applications is generally accepted, even with potential exposure to rainfall or stormwater, as long as the materials do not pose a risk to groundwater or surface water. A thorough environmental risk assessment is necessary to ensure the safe application of WBP and GGBS blends, as well as MG-45S-55B and CG-45S-55B geopolymers in various engineering projects. Table 3 presents the leachate analysis results of WBP, GGBS, and the two geopolymers using acetic leachate extraction. This analysis helps determine the potential for harmful substances to leach from these materials into the surrounding environment. The US Environmental Protection Agency (EPA) provides guidelines and thresholds for hazardous waste identification based on leachate analysis [91]. Wartman et al. [92] clarified that according to the EPA a material is considered hazardous waste if any detected metal exceeds 100 times the drinking water standards.

Comparing the leachate test results with EPA limits, it is evident that all metal contaminants in the WBP, GGBS, and geopolymer samples fall within acceptable limits. Moreover, the results indicate that the MG-45S-55B and CG-45S-55B geopolymers effectively reduce the leachability of certain metals, specifically arsenic and zinc. This reduction is attributed to the geopolymer's unique structure, which consists of a three-dimensional framework of SiO_4 and AlO_4 tetrahedra, primarily composed of SiO_2, Al_2O_3, and Fe_2O_3. This framework carries a net negative charge, balanced by exchangeable cations [93–95]. Metal ion uptake is primarily facilitated by ion exchange reactions within microporous zeolite-like minerals present in geopolymers [96,97]. This important finding strongly indicates that the solidified samples, after undergoing the stabilization process and curing period, do not pose a significant environmental hazard.

4. Conclusions

This work was centered on investigating the behavior of geopolymer grout's mechanochemical activation in contrast to its traditional activation. The impact of substituting GGBS with WBP was evaluated using three new properties: microstructure properties (SEM analysis), mechanical properties (UCS), and fresh properties (mini-slump flow and setting time). The conclusions were as follows:

- The SEM images demonstrated that the MG powder's particle size decreased following grinding and their shape changed. This increased particle surface area led to the formation of more alumina and silica, further enhancing the geopolymer grout MG powder.

- The presence of full WBP reduced the workability of geopolymer grout. However, the inclusion of GGBS as a partial substitute for WBP in the geopolymer grout noticeably improved its workability. The substitution of 15–45% GGBS with the WBP-geopolymer-based grout

increased the slump flow of MG grouts by 10–27%. In addition, the results demonstrated that the activation method (mechanochemical activation) affected the slump flow of the geopolymer grout. The slump flow ranged from 85 to 110 mm for the MG mixtures and 105–130 mm for the CG mixtures.

- The contribution of 15–45% GGBS in the mixture of WRP-based geopolymers caused a significant reduction in the final setting time, i.e., from 235 to 90 min each. This significant reduction was caused by mechanochemical activation. The final setting times for CG and MG were 255 and 235 min, respectively.

- The results demonstrate that substituting the WBP with GGBS resulted in a linear enhancement in strength as the amount of GGBS used increased. The UCS values of the geopolymer mix demonstrated increases of 90, 174, and 227% when the WBP was substituted with 15, 30, and 45% GGBS, respectively.

- The MG samples showed 7–30% higher UCS values compared to those of the CG samples. The mechanochemical activation process can be attributed to this improvement, which increased both the reaction rate and the surface area. Resultantly, an additional gel was formed, accumulating and filling the pore system and finally enhancing the MG grout's strength.

- Based on the SEM images, the geopolymer samples with 45% GGBS are more structurally compact and homogeneous, with produced gels and lesser non-reactive particles than those with 100% WBP, which are more microstructurally porous and less cohesive. Meanwhile, GGBS' amorphous nature, as shown by the XRD test, increased the alkali activation reaction rate, thus intensifying the production of C–S–H and C–A–S–H and increasing the strength.

- Based on the microstructure analysis results, the geopolymer grout's microstructure is substantially impacted by the activation method as a result of the grinding process, increasing the GGBS and WBP surface area, lessening the particle size, and ultimately producing geopolymer grout samples that are less porous and denser compared to the conventionally activated samples.

5. Future research directions

- **Comprehensive cost-benefit analysis**: Detailed studies on the energy consumption, operational costs, and scalability of mechanochemical activation are essential to evaluate its economic feasibility for large-scale construction projects.

- **Expanded durability testing**: Future research should explore MG grouts under diverse and dynamic environmental conditions, such as variable moisture levels, freeze–thaw cycles, and acid attack, to develop predictive models for long-term performance.

- **Microstructural evolution**: Advanced microstructural characterization, including phase analysis and pore structure evolution, will provide insights into the mechanisms underlying MG grouts' mechanical performance and durability.

- **Environmental impact assessment**: The leaching behavior of potentially hazardous elements, carbon footprint analysis, and compliance with environmental regulations need to be thoroughly investigated to ensure sustainable application.

- **Field-scale validation:** Scaling up laboratory findings to field conditions is critical. Pilot studies incorporating varied soil types, construction practices, and environmental conditions will validate the real-world applicability of MG grouts.

- **Comparative studies:** Direct comparisons of MG grouts with conventional soil stabilization methods in terms of cost, environmental impact, mechanical performance, and durability are necessary to highlight the unique advantages and limitations of this approach.

- **Lifecycle analysis:** Conducting a lifecycle assessment will help quantify the environmental and economic sustainability of MG grouts across their production, application, and disposal phases.

Acknowledgements

To my father. This achievement is a tribute to his enduring influence and the love he so selflessly gave. Forever grateful, forever in my heart.

Author contributions

Altug Saygılı: Supervision, Reviewing and Editing, Validation. Ahmed Ali Agha: Conceptualization, Writing

– Original draft preparation, Methodology, Software, Investigation. Mukhtar Hamid Abed: Data curation, Investigation, Writing-Reviewing and Editing.

Conflict of interest statement

The authors declare that they have no known competing financial interests or personal relationships that could have appeared to influence the work reported in this paper.

Data availability statement

All data from experiments that support the findings of this study are available from the corresponding author upon request.

References

[1] Amer, A.A., El-Hoseny, S., Properties and performance of metakaolin pozzolanic cement pastes, J. Therm. Anal. Calorim., 2017, 129: 33–44. doi: 10.1007/s10973-017-6087-9

[2] Rios, S., Ramos, C., Viana da Fonseca, A., Cruz, N., Rodrigues, C., Mechanical and durability properties of a soil stabilised with an alkali-activated cement, Eur. J. Environ. Civ. Eng., 2019, 23: 245–267. doi: 10.1080/19648189.2016.1275987

[3] Duxson, P., Fernández-Jiménez, A., Provis, J.L., Lukey, G.C., Palomo, A., Van Deventer, J.S.J., Geopolymer technology: The current state of the art, J. Mater. Sci., 2007, 42: 2917–2933. doi: 10.1007/s10853-006-0637-z

[4] Lee, W.K.W., Van Deventer, J.S.J., The effect of ionic contaminants on the early-age properties of alkali-activated fly ash-based cements, Cem. Concr. Res., 2002, 32: 577–584

[5] Zhang, M., Guo, H., El-Korchi, T., Zhang, G., Tao, M., Experimental feasibility study of geopolymer as the next-generation soil stabilizer, Constr. Build. Mater., 2013, 47: 1468–1478

[6] Yaghoubi, M., Arulrajah, A., Miri Disfani, M., Horpibulsuk, S., Leong, M., Compressibility and strength development of geopolymer stabilized columns cured under stress, Soils Found., 2020, 60: 1241–1250. doi: 10.1016/j.sandf.2020.07.005

[7] Palomo, A., Blanco-Varela, M.T., Granizo, M.L., Puertas, F., Vazquez, T., Grutzeck, M.W., Chemical stability of cementitious materials based on metakaolin, Cem. Concr. Res., 1999, 29: 997–1004

[8] Cheng, T.W., Chiu, J.P., Fire-resistant geopolymer produced by granulated blast furnace slag, Miner. Eng., 2003, 16: 205–210

[9] Zhang, H.Y., Liu, J.C., Wu, B., Mechanical properties and reaction mechanism of one-part geopolymer mortars, Constr. Build. Mater., 2021, 273: 121973. doi: 10.1016/j.conbuildmat.2020.121973

[10] Lee, W.K.W., Van Deventer, J.S.J., Structural reorganisation of class F fly ash in alkaline silicate solutions, Colloids Surf. A: Physicochem. Eng. Asp., 2002, 211: 49–66

[11] Lee, W.K.W., Van Deventer, J.S.J., Use of infrared spectroscopy to study geopolymerization of heterogeneous amorphous aluminosilicates, Langmuir, 2003, 19: 8726–8734. doi: 10.1021/la026127e

[12] Nematollahi, B., Sanjayan, J., Shaikh, F.U.A., Synthesis of heat and ambient cured one-part geopolymer mixes with different grades of sodium silicate, Ceram. Int., 2015, 41: 5696–5704

[13] Abbas, I.S., Abed, M.H., Canakci, H., Development and characterization of eco-and user-friendly grout production via mechanochemical activation of geopolymer, J. Build. Eng., 2022, 63: 105336

[14] Hamid Abed, M., Abbas, I.S., Canakci, H., Influence of mechanochemical activation on the rheological, fresh, and mechanical properties of one-part geopolymer grout, Adv. Cem. Res., 2022, 35: 1–38

[15] Matalkah, F., Xu, L., Wu, W., Soroushian, P., Mechanochemical synthesis of one-part alkali aluminosilicate hydraulic cement, Mater. Struct., 2017, 50: 1–12. doi: 10.1617/s11527-016-0968-4

[16] Guo, X., Xiang, D., Duan, G., Mou, P., A review of mechanochemistry applications in waste management, Waste Manag.., 2010, 30: 4–10. doi: 10.1016/j.wasman.2009.08.017

[17] Hosseini, S., Brake, N.A., Nikookar, M., Günaydın-Şen, Ö., Snyder, H.A., Mechanochemically activated bottom ash-fly ash geopolymer, Cem. Concr. Compos., 2021, 118: 103976. doi: 10.1016/j.cemconcomp.2021.103976

[18] Gupta, R., Bhardwaj, P., Mishra, D., Mudgal, M., Chouhan, R.K., Prasad, M., et al., Evolution of advanced geopolymeric cementitious material via a novel process, Adv. Cem. Res., 2017, 29: 125–134. doi: 10.1680/jadcr.16.00113

[19] Mudgal, M., Chouhan, R.K., Kushwah, S., Srivastava, A.K., Enhancing reactivity and properties of fly-ash-based solid-form geopolymer via ball-milling, Emerg. Mater. Res., 2019, 9: 2–9

[20] Kumar, S., Kumar, R., Mechanical activation of fly ash: Effect on reaction, structure and properties of resulting geopolymer, Ceram. Int., 2011, 37: 533–541
[21] Migunthanna, J., Rajeev, P., Sanjayan, J., Investigation of waste clay brick as partial replacement in geopolymer binder, Constr. Build. Mater., 2023, 365: 130107. doi: 10.1016/j.conbuildmat.2022.130107
[22] Sharmin, S., Sarker, P.K., Biswas, W.K., Abousnina, R.M., Javed, U., Characterization of waste clay brick powder and its effect on the mechanical properties and microstructure of geopolymer mortar, Constr. Build. Mater., 2024, 412: 134848. doi: 10.1016/j.conbuildmat.2023.134848
[23] Wong, C.L., Mo, K.H., Alengaram, U.J., Yap, S.P., Mechanical strength and permeation properties of high calcium fly ash-based geopolymer containing recycled brick powder, J. Build. Eng., 2020, 32: 101655. doi: 10.1016/j.jobe.2020.101655
[24] Ye, T., Xiao, J., Duan, Z., Li, S., Geopolymers made of recycled brick and concrete powder – A critical review, Constr. Build. Mater., 2022, 330: 127232. doi: 10.1016/j.conbuildmat.2022.127232
[25] Wang, B., Yan, L., Fu, Q., Kasal, B., A comprehensive review on recycled aggregate and recycled aggregate concrete, Resour. Conserv. Recycl., 2021, 171: 105565. doi: 10.1016/j.resconrec.2021.105565
[26] Tang, Q., Ma, Z., Wu, H., Wang, W., The utilization of eco-friendly recycled powder from concrete and brick waste in new concrete: A critical review, Cem. Concr. Compos., 2020, 114: 103807. doi: 10.1016/j.cemconcomp.2020.103807
[27] Abadel, A.A., Alghamdi, H., Effect of high volume tile ceramic wastes on resistance of geopolymer mortars to abrasion and freezing-thawing cycles: Experimental and deep learning modelling, Ceram. Int., 2023, 49: 15065–15081. doi: 10.1016/j.ceramint.2023.01.089
[28] Albidah, A., Abadel, A., Alrshoudi, F., Altheeb, A., Abbas, H., Al-Salloum, Y., Bond strength between concrete substrate and metakaolin geopolymer repair mortars at ambient and elevated temperatures, J. Mater. Res. Technol., 2020, 9: 10732–10745. doi: 10.1016/j.jmrt.2020.07.092
[29] Naceri, A., Hamina, M.C., Use of waste brick as a partial replacement of cement in mortar, Waste Manag., 2009, 29: 2378–2384. doi: 10.1016/j.wasman.2009.03.026
[30] Figiela, B., Brudny, K., Lin, W.T., Korniejenko, K., Investigation of mechanical properties and microstructure of construction-and demolition-waste-based geopolymers, J. Compos. Sci., 2022, 6: 191. doi: 10.3390/jcs6070191
[31] Alghamdi, H., Abadel, A.A., Khawaji, M., Alamri, M., Alabdulkarim, A., Strength performance and microstructures of alkali-activated metakaolin and GGBFS-based mortars: role of waste red brick powder incorporation, Minerals, 2023, 13: 848.
[32] Abadel, A.A., Alghamdi, H., Alharbi, Y.R., Alamri, M., Khawaji, M., Abdulaziz, M.A.M., et al., Investigation of alkali-activated slag-based composite incorporating dehydrated cement powder and red mud, Materials (Basel), 2023, 16: 1551
[33] Rakhimova, N.R., Rakhimov, R.Z., Alkali-activated cements and mortars based on blast furnace slag and red clay brick waste, Mater. Des., 2015, 85: 324–331. doi: 10.1016/j.matdes.2015.06.182
[34] Zhu, L., Zhu, Z., Reuse of clay brick waste in mortar and concrete, Adv. Mater. Sci. Eng.., 2020, 2020: 6326178. doi: 10.1155/2020/6326178
[35] Xiao, J., Ma, Z., Sui, T., Akbarnezhad, A., Duan, Z., Mechanical properties of concrete mixed with recycled powder produced from construction and demolition waste, J. Clean. Prod., 2018, 188: 720–731. doi: 10.1016/j.jclepro.2018.03.277
[36] Mahmoodi, O., Siad, H., Lachemi, M., Sahmaran, M., Synthesis and optimization of binary systems of brick and concrete wastes geopolymers at ambient environment, Constr. Build. Mater., 2021, 276: 122217. doi: 10.1016/j.conbuildmat.2020.122217
[37] Marjanović, N., Komljenović, M., Baščarević, Z., Nikolić, V., Petrović, R., Physical-mechanical and microstructural properties of alkali-activated fly ash-blast furnace slag blends, Ceram. Int., 2015, 41: 1421–1435. doi: 10.1016/j.ceramint.2014.09.075
[38] Palacios, M., Gismera, S., Alonso, M.M., d'Espinose de Lacaillerie, J.B., Lothenbach, B., Favier, A., et al., Early reactivity of sodium silicate-activated slag pastes and its impact on rheological properties, Cem. Concr. Res., 2021, 140: 106302. doi: 10.1016/j.cemconres.2020.106302
[39] Lu, C., Zhang, Z., Shi, C., Li, N., Jiao, D., Yuan, Q., Rheology of alkali-activated materials: A review, Cem. Concr. Compos., 2021, 121: 104061. doi: 10.1016/j.cemconcomp.2021.104061
[40] Ye, H., Radlińska, A., Shrinkage mitigation strategies in alkali-activated slag, Cem. Concr. Res., 2017, 101: 131–143. doi: 10.1016/j.cemconres.2017.08.025
[41] Ye, H., Radlińska, A., Shrinkage mechanisms of alkali-activated slag, Cem. Concr. Res., 2016, 88: 126–135. doi: 10.1016/j.cemconres.2016.07.001
[42] Hojati, M., Radlin, A., Radlińska, A., Shrinkage and strength development of alkali-activated fly ash-

slag binary cements, Constr. Build. Mater., 2017, 150: 808–816. doi: 10.1016/j.conbuildmat.2017.06.040

[43] Zawrah, M.F., Gado, R.A., Feltin, N., Ducourtieux, S., Devoille, L., Recycling and utilization assessment of waste fired clay bricks (Grog) with granulated blast-furnace slag for geopolymer production, Process. Saf. Environ. Prot., 2016, 103: 237–251. doi: 10.1016/j.psep.2016.08.001

[44] Fořt, J., Novotný, R., Vejmelková, E., Trník, A., Rovnaníková, P., Keppert, M., et al., Characterization of geopolymers prepared using powdered brick, J. Mater. Res. Technol., 2019, 8: 6253–6261. doi: 10.1016/j.jmrt.2019.10.019

[45] Abed, F.H., Zareei, S.A., Kurdi, N.H., Emami, A., Enhancing geopolymer binder reactivity and performance via mechanochemical activation: A comprehensive study of rheological, mechanical, and microstructural properties, Constr. Build. Mater., 2024, 430: 136456. doi: 10.1016/j.conbuildmat.2024.136456

[46] Hamid Abed, M., Sabbar Abbas, I., Hamed, M., Canakci, H., Rheological, fresh, and mechanical properties of mechanochemically activated geopolymer grout: A comparative study with conventionally activated geopolymer grout, Constr. Build. Mater., 2022, 322: 126338. doi: 10.1016/j.conbuildmat.2022.126338

[47] Raghuraman, P., Raman, R.R., Pitchumani, B., Studies in fine grinding in an attritor mill, In: Developments in mineral processing, Elsevier, 2000, pp. C4–C94

[48] Ilcan, H., Sahin, O., Kul, A., Yildirim, G., Sahmaran, M., Rheological properties and compressive strength of construction and demolition waste-based geopolymer mortars for 3D-Printing, Constr. Build. Mater., 2022, 328: 127114

[49] Mahmoodi, O., Siad, H., Lachemi, M., Dadsetan, S., Sahmaran, M., Optimization of brick waste-based geopolymer binders at ambient temperature and pre-targeted chemical parameters, J. Clean. Prod., 2020, 268: 122285. doi: 10.1016/j.jclepro.2020.122285

[50] Kantro, D.L., Influence of water-reducing admixtures on properties of cement paste – a miniature slump test, Cem. Concr. Aggreg., 1980, 2: 95–102

[51] Güllü, H., Ali Agha, A., The rheological, fresh and strength effects of cold-bonded geopolymer made with metakaolin and slag for grouting, Constr. Build. Mater., 2021, 274: 122091. doi: 10.1016/j.conbuildmat.2020.122091

[52] ASTM, C. Standard test methods for time of setting of hydraulic cement by Vicat needle. ASTM International, West Conshohocken, PA, 2008, C191-08

[53] Astm, C. 942. Standard test method for compressive strengths of grouts for preplaced-aggregate concrete in the laboratory, Annual Book of ASTM Standards, 2008.

[54] ASTM, A. Standard test method of unconfined compressive strength of intact rock core specimens, ASTM Publication, 1986.

[55] Amini, O., Ghasemi, M., Laboratory study of the effects of using magnesium slag on the geotechnical properties of cement stabilized soil, Constr. Build. Mater., 2019, 223: 409–420

[56] Baalamurugan, J., Ganesh Kumar, V., Stalin Dhas, T., Taran, S., Nalini, S., Karthick, V., et al., Utilization of induction furnace steel slag based iron oxide nanocomposites for antibacterial studies, SN Appl. Sci., 2021, 3: 1–8. doi: 10.1007/s42452-021-04299-9

[57] Hwang, C.L., Damtie Yehualaw, M., Vo, D.H., Huynh, T.P., Development of high-strength alkali-activated pastes containing high volumes of waste brick and ceramic powders, Constr. Build. Mater., 2019, 218: 519–529. doi: 10.1016/j.conbuildmat.2019.05.143

[58] Hamid Abed, M., Hamid Abed, F., Alireza Zareei, S., Sabbar Abbas, I., Canakci, H., Kurdi, N.H., et al., Experimental feasibility study of using eco- and user-friendly mechanochemically activated slag/fly ash geopolymer for soil stabilization, Clean. Mater., 2024, 11: 100226. doi: 10.1016/j.clema.2024.100226

[59] Chen, M.Z., Lin, J.T., Wu, S.P., Liu, C.H., Utilization of recycled brick powder as alternative filler in asphalt mixture, Constr. Build. Mater., 2011, 25: 1532–1536. doi: 10.1016/j.conbuildmat.2010.08.005

[60] Wang, Y., Wang, M., Wang, H., Dun, Z., Ren, L., Experimental research on application of waste concrete powder–waste brick powder–cement grout for foundation reinforcement in mining goaf, Materials (Basel), 2023, 16: 6075. doi: 10.3390/ma16186075

[61] Ahmed, J.K., Atmaca, N., Khoshnaw, G.J., Building a sustainable future: An experimental study on recycled brick waste powder in engineered geopolymer composites, Case Stud. Constr. Mater., 2024, 20: e02863. doi: 10.1016/j.cscm.2024.e02863

[62] ASTM International. ASTM C1437-15 Standard test method for flow of hydraulic cement mortar, ASTM International, West Conshohocken, PA, USA, 2015.

[63] Hamid Abed, M., Hamid Abed, F., Alireza Zareei, S., Sabbar Abbas, I., Canakci, H., Kurdi, N.H., et al., Experimental feasibility study of eco- and user-friendly mechanochemically activated slag/fly ash

geopolymer for soil stabilization, Clean. Mater., 2024, 11: 100226. doi: 10.1016/j.clema.2024.100226

[64] Hamid Abed, M., Hamid Abed, F., Zareei, S.A., Abbas, I.S., Canakci, H., Kurdi, N.H., Mechanical and durability performance of eco-friendly geopolymer-stabilized soil, Proc. Inst. Civ. Eng. Gr. Improv., 2024, 1–17. doi: 10.1680/jgrim.23.00037

[65] Abed, M.H., Abbas, I.S., Development and assessment of eco- and user-friendly geopolymeric stabilizers for sustainable soil improvement, Clean. Waste Syst., 2024, 9: 100170. doi: 10.1016/j.clwas.2024.100170

[66] Zhang, J., Li, S., Li, Z., Zhang, Q., Li, H., Du, J., et al., Properties of fresh and hardened geopolymer-based grouts, Ceram. Silik., 2019, 63: 164–173. doi: 10.13168/cs.2019.0008

[67] Abou-Zeid, M., Fowler, D.W., Nawy, E.G., Allen, J.H., Halvorsen, G.T., Poston, R.W., et al., Control of cracking in concrete structures, Rep. ACI Comm.., 2001, 224: 12–16

[68] Samantasinghar, S., Singh, S.P., Fresh and hardened properties of fly ash–slag blended geopolymer paste and mortar, Int. J. Concr. Struct. Mater., 2019, 13: 1–12. doi: 10.1186/s40069-019-0360-1

[69] Nath, P., Sarker, P.K., Effect of GGBFS on setting, workability and early strength properties of fly ash geopolymer concrete cured in ambient condition, Constr. Build. Mater., 2014, 66: 163–171

[70] Kumar, S., Kumar, R., Mehrotra, S.P., Influence of granulated blast furnace slag on the reaction, structure and properties of fly ash based geopolymer, J. Mater. Sci., 2010, 45: 607–615. doi: 10.1007/s10853-009-3934-5

[71] Kato, K., Xin, Y., Hitomi, T., Shirai, T., Surface modification of fly ash by mechano-chemical treatment, Ceram. Int., 2019, 45: 849–853. doi: 10.1016/j.ceramint.2018.09.254

[72] Li, H., Xu, D., Feng, S., Shang, B., Microstructure and performance of fly ash micro-beads in cementitious material system, Constr. Build. Mater., 2014, 52: 422–427. doi: 10.1016/j.conbuildmat.2013.11.040

[73] Marjanović, N., Komljenović, M., Baščarević, Z., Nikolić, V., Improving reactivity of fly ash and properties of ensuing geopolymers through mechanical activation, Constr. Build. Mater., 2014, 57: 151–162. doi: 10.1016/j.conbuildmat.2014.01.095

[74] Tho-In, T., Sata, V., Boonserm, K., Chindaprasirt, P., Compressive strength and microstructure analysis of geopolymer paste using waste glass powder and fly ash, J. Clean. Prod., 2016, 172: 2892–2898. doi: 10.1016/j.jclepro.2017.11.125

[75] Liang, G., Zhu, H., Zhang, Z., Wu, Q., Du, J., Investigation of the waterproof property of alkali-activated metakaolin geopolymer added with rice husk ash, J. Clean. Prod., 2019, 230: 603–612. doi: 10.1016/j.jclepro.2019.05.111

[76] Athira, V.S., Bahurudeen, A., Saljas, M., Jayachandran, K., Influence of different curing methods on mechanical and durability properties of alkali activated binders, Constr. Build. Mater., 2021, 299: 123963. doi: 10.1016/j.conbuildmat.2021.123963

[77] Fořt, J., Mildner, M., Keppert, M., Pommer, V., Černý, R., Experimental and environmental analysis of high-strength geopolymer based on waste bricks and blast furnace slag, Polymers (Basel), 2023, 15: 3092. doi: 10.3390/polym15143092

[78] Nath, S.K., Kumar, S., Influence of iron making slags on strength and microstructure of fly ash geopolymer, Constr. Build. Mater., 2013, 38: 924–930. doi: 10.1016/j.conbuildmat.2012.09.070

[79] Nath, S.K., Kumar, S., Influence of granulated silico-manganese slag on compressive strength and microstructure of ambient cured alkali-activated fly ash binder, Waste Biomass Valoriz., 2019, 10: 2045–2055. doi: 10.1007/s12649-018-0213-1

[80] Ma, Y., Hu, J., Ye, G., The pore structure and permeability of alkali activated fly ash, Fuel, 2013, 104: 771–780. doi: 10.1016/j.fuel.2012.05.034

[81] Zheng, L., Wang, W., Shi, Y., The effects of alkaline dosage and Si/Al ratio on the immobilization of heavy metals in municipal solid waste incineration fly ash-based geopolymer, Chemosphere, 2010, 79: 665–671. doi: 10.1016/j.chemosphere.2010.02.018

[82] Zhang, J., Provis, J.L., Feng, D., van Deventer, J.S.J., Geopolymers for immobilization of Cr^{6+}, Cd^{2+}, and Pb^{2+}, J. Hazard. Mater., 2008, 157: 587–598. doi: 10.1016/j.jhazmat.2008.01.053

[83] Izquierdo, M., Querol, X., Davidovits, J., Antenucci, D., Nugteren, H., Fernández-Pereira, C., Coal fly ash-slag-based geopolymers: Microstructure and metal leaching, J. Hazard. Mater., 2009, 166: 561–566. doi: 10.1016/j.jhazmat.2008.11.063

[84] Provis, J.L., Myers, R.J., White, C.E., Rose, V., Van Deventer, J.S.J., X-ray microtomography shows pore structure and tortuosity in alkali-activated binders, Cem. Concr. Res., 2012, 42: 855–864. doi: 10.1016/j.cemconres.2012.03.004

[85] Hamid, M., Abbas, I.S., Canakci, H., Effect of glass powder on the rheological and mechanical proper-

ties of slag-based mechanochemical activation geopolymer grout, Eur. J. Environ. Civ. Eng., 2022, 27: 1–25. doi: 10.1080/19648189.2022.2145374

[86] Wang, W., Wu, H., Ma, Z., Wu, R., Using eco-friendly recycled powder from CDW to prepare strain hardening cementitious composites (SHCC) and properties determination, Materials (Basel), 2020, 13: 1143. doi: 10.3390/ma13051143

[87] Ismail, I., Bernal, S.A., Provis, J.L., San Nicolas, R., Hamdan, S., Van Deventer, J.S.J., Modification of phase evolution in alkali-activated blast furnace slag by the incorporation of fly ash, Cem. Concr. Compos., 2014, 45: 125–135. doi: 10.1016/j.cemconcomp.2013.09.006

[88] Gupta, R., Bhardwaj, P., Mishra, D., Prasad, M., Amritphale, S.S., Formulation of mechanochemically evolved fly ash based hybrid inorganic–organic geopolymers with multilevel characterization, J. Inorg. Organomet. Polym. Mater., 2017, 27: 385–398. doi: 10.1007/s10904-016-0461-0

[89] Gupta, R., Bhardwaj, P., Deshmukh, K., Mishra, D., Prasad, M., Amritphale, S.S., Development and characterization of inorganic-organic (Si-O-Al) hybrid geopolymeric precursors via solid state method, Silicon, 2019, 11: 221–232

[90] Navrátilová, E., Rovnaníková, P., Pozzolanic properties of brick powders and their effect on the properties of modified lime mortars, Constr. Build. Mater., 2016, 120: 530–539. doi: 10.1016/j.conbuildmat.2016.05.062

[91] U.S. Epa, National primary drinking water standards, Off. Water, United States Environ. Prot. Agency, Washington, DC, 2003

[92] Wartman, J., Grubb, D.G., Nasim, A.S.M., Select engineering characteristics of crushed glass, J. Mater. Civ. Eng., 2004, 16: 526–539

[93] Cheng, K.Y., Bishop, P., Metals distribution in solidified/stabilized waste forms after leaching, Hazard. Waste Hazard. Mater., 1992, 9: 163–171

[94] Napia, C., Sinsiri, T., Jaturapitakkul, C., Chindaprasirt, P., Leaching of heavy metals from solidified waste using Portland cement and zeolite as a binder, Waste Manag.., 2012, 32: 1459–1467

[95] Peralta, G.L., Ballesteros, F., Cepeda, M., Treatment and disposal of heavy metal waste using cementitious solidification, In: PACIFIC BASIN, Conference On Hazardous Waste, 1992

[96] Erdem, E., Karapinar, N., Donat, R., The removal of heavy metal cations by natural zeolites, J. Colloid Interface Sci., 2004, 280: 309–314

[97] Abed, M.H., Abbas, I.S., Mohmmad, S.H., Saygili, A., Agha, A.A., Performance of soils stabilized with eco-friendly mechanochemical geopolymeric activators, Geotech. Geol. Eng., 2025, 43: 117. doi: 10.1007/s10706-025-03073-7.